

Rashba spin-orbit interaction in a $\text{Mg}_x\text{Zn}_{1-x}\text{O}/\text{ZnO}$ two-dimensional electron gas studied by electrically detected electron spin resonance

Y. Kozuka,^{1,*} S. Teraoka,¹ J. Falson,¹ A. Oiwa,¹ A. Tsukazaki,^{1,2} S. Tarucha,^{1,3,4} and M. Kawasaki^{1,3}

¹*Department of Applied Physics and Quantum-Phase Electronics Center (QPEC), University of Tokyo, Tokyo 113-8656, Japan*

²*PRESTO, Japan Science and Technology Agency (JST), Tokyo 102-0075, Japan*

³*Center for Emergent Matter Science (CEMS), RIKEN, Wako, Saitama 351-0198, Japan*

⁴*INQIE, University of Tokyo, Tokyo 153-8505, Japan*

(Received 30 January 2013; published 7 May 2013)

We report the experimental determination of Rashba spin-orbit interaction (SOI) strength in two-dimensional electrons in a MgZnO/ZnO heterostructure using electrically detected electron spin resonance. The Rashba parameter is determined to be 7.0×10^{-14} eV m, which is the second smallest value among prevalent semiconductor heterostructures, following Si/SiGe. A long transverse spin relaxation time was derived to show a maximum value of 27 ns, owing to weak SOI. Our study demonstrates that the ZnO heterostructure is a promising candidate for spintronic devices utilizing long spin coherence.

DOI: [10.1103/PhysRevB.87.205411](https://doi.org/10.1103/PhysRevB.87.205411)

PACS number(s): 75.70.Tj, 72.25.Rb, 73.23.-b, 73.43.-f

I. INTRODUCTION

Extensive progress has recently been made in the field of semiconductor spintronics, which primarily focuses on the generation, manipulation, and detection of electron spins.¹⁻³ Transporting spin information is also a fundamental prerequisite to bridge these three operations. In order to reconcile these requirements, Rashba spin-orbit interaction (SOI) has attracted much attention because it enables the former three operations, and simultaneously, the strength is electrically tunable.⁴⁻⁷ Such tunability is preferable, as Rashba SOI is also a source of spin dephasing, via the D'yakonov-Perel' (DP) mechanism.⁸ Since Rashba SOI is triggered by the internal electric field transverse to the electron motion, (In,Ga)As-based heterostructures with asymmetric potential profiles have been extensively investigated for spin manipulation.^{5,9} Although these studies demonstrated the high potential to control Rashba SOI, the inherent high density (almost 100%) of nuclear spins in the GaAs host material are found to destruct the electron spin coherence, limiting the capability of preserving spin information.¹⁰ Only recently have Si/SiGe heterostructures been intensively investigated for quantum information application due to the natural abundance as low as 4% for Si isotopes having a 1/2 nuclear spin.¹¹

As this field is still developing, it is important to broaden the range of host materials beyond well-developed semiconductors such as GaAs and Si. In terms of long spin coherence time, ZnO is another promising material, where only ⁶⁷Zn, which exist naturally as 4% among Zn isotopes, possesses a 5/2 nuclear spin, and extremely weak SOI is also theoretically predicted.¹² Another advantage of ZnO in designing practical device structure is that the conduction band consists of single parabolic band at the Γ point in contrast to multivalley band structure of Si. In addition, recent rapid advances in the growth technique of ZnO heterostructures enhance the feasibility of practical device fabrication. In the MgZnO/ZnO heterostructures, a two-dimensional electron gas (2DEG) is spontaneously formed at the interface without remote doping of donors due to the polarization mismatch of the buffer and capping layer.¹³ State-of-the-art samples now show an electron mobility as high as $700\,000\text{ cm}^2\text{ V}^{-1}\text{ s}^{-1}$ and a mean free path as long as $5\ \mu\text{m}$, enabling the clear observation of multiple fractional quantum

Hall states.^{14,15} Given such a platform, it is timely to examine the feasibility of this system for quantum devices.^{16,17} In spite of such promising properties, Rashba SOI or spin relaxation in the MgZnO/ZnO 2DEG has never been investigated. In fact, beating of Shubnikov-de Haas oscillations (SdH)⁵ or weak antilocalization,^{12,18} which has been frequently used to estimate the strength of SOI, has never been observed in ZnO, probably because the weak SOI cannot give rise to sufficient perturbation to steady-state transport properties.¹²

Here we report on the study of electrically detected electron spin resonance (ESR) in a MgZnO/ZnO heterostructure. This technique detects the Zeeman splitting energy through microwave (MW) irradiation under magnetic field and has been utilized to detect extremely small Rashba SOI in Si/SiGe heterostructures from a perturbation to the splitting energy¹⁹ because of its high sensitivity and high accuracy of the resonance energy.¹⁰ In this study we successfully observed ESR signals in a MgZnO/ZnO heterostructure, which enabled us to precisely determine the spin splitting energy and thus to estimate the Rashba SOI strength. The obtained Rashba parameter (α) is found to be as small as 7.0×10^{-14} eV m, which follows the smallest α value of 5.5×10^{-15} eV m in Si/SiGe heterostructures.¹⁹ The collective transverse spin relaxation time (T_2^*) was also estimated from the full width at half maximum (FWHM) of the resonance peaks, which shows a maximum value of 27 ns. Our results provide the first experimental determination of the Rashba SOI strength and spin relaxation time of the high-mobility 2DEG in a MgZnO/ZnO heterostructure.

II. EXPERIMENT

The MgZnO/ZnO heterostructure was fabricated by molecular beam epitaxy using high-purity 7 N Zn and 6 N Mg metals together with distilled pure ozone as the oxygen source.¹⁵ The film was patterned into Hall-bar geometry by ion milling, followed by Ti evaporation for Ohmic electrodes. With Al wire ultrasonically bonded, the sample was placed at the end of a MW cavity, which was connected to a MW source through a semirigid coaxial cable, and was cooled in a ³He cryostat equipped with 9 T superconducting magnet.

The resistance of the sample was measured by a conventional lock-in technique with an excitation current of 100 nA modulated at a frequency of 13 Hz. The ESR signal was detected as a change in longitudinal resistance in response to MW irradiation (ΔR_{xx}) since the absorbed MW sensitively affects the 2DEG resistance. Instead of directly measuring ΔR_{xx} , we employed a double lock-in technique under an MW amplitude modulation with a frequency of ~ 1 kHz to enhance the sensitivity as explained in Ref. 20. Below we show the results at a fixed temperature of 0.25 K and a MW intensity on the order of 0.1 mW. Although ESR signals are reduced with increasing temperature or with decreasing MW intensity, the resonance magnetic fields and the peak widths, which we focus on, are found to be independent of these conditions.

III. RESULTS AND DISCUSSIONS

We first measured the magnetic field (B) dependence of longitudinal resistance (R_{xx}) and Hall resistance (R_{xy}) without

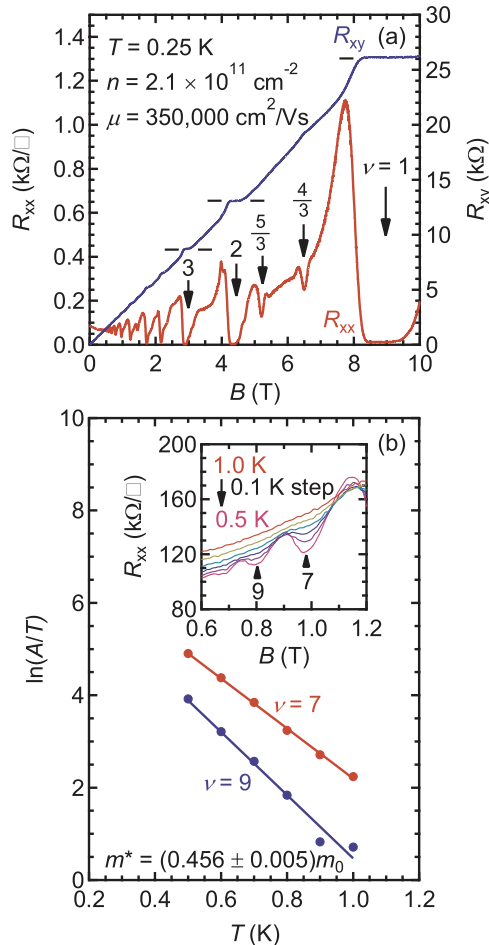


FIG. 1. (Color online) (a) Magnetic field dependence of longitudinal resistance (R_{xx}) and Hall resistance (R_{xy}) for the MgZnO/ZnO heterostructure measured at 0.25 K. (b) Temperature dependence of Shubnikov–de Haas amplitude (A) divided by temperature for filling factors of $\nu = 7$ and 9, which leads to an effective mass value of $m^* = (0.456 \pm 0.005)m_0$. The solid lines are the fits to the data for estimating m^* . The inset shows Shubnikov–de Haas oscillations at several temperatures from 0.5 to 1.0 K.

MW irradiation at 0.25 K as shown in Fig. 1(a), which exhibits clear integer and fractional quantum Hall states. Neither beating of SdH nor weak antilocalization is present, evidencing negligibly small SOI. The carrier density (n) and the mobility (μ) of the sample are $2.1 \times 10^{11} \text{ cm}^{-2}$ and $350\,000 \text{ cm}^2 \text{ V}^{-1} \text{ s}^{-1}$, respectively. The effective mass was also estimated as $(0.456 \pm 0.005)m_0$ (m_0 is the free electron mass) from the temperature dependence of SdH oscillations as shown in the inset of Fig. 1(b). Here the oscillation amplitude (A) was fitted with a mathematical expression of $A/R_0 = 4\chi \exp(-\pi/\omega_c \tau_q) / \sinh \chi$ as in Fig. 1(b), where R_0 is the resistance at $B = 0$ T, χ represents $2\pi^2 k_B T / \hbar \omega_c$ (k_B is the Boltzmann constant), $\omega_c = eB/m^*$ is the cyclotron frequency, and τ_q is the quantum scattering time.²¹

Upon the irradiation of MW, sharp peaks were observed in ΔR_{xx} as shown in Fig. 2(a) at a resonant magnetic field (B_{res}) corresponding to ESR condition of $\hbar \omega = g^* \mu_B B_{\text{res}}$, where \hbar is the Planck constant divided by 2π , $\omega = 2\pi f$ is the angular

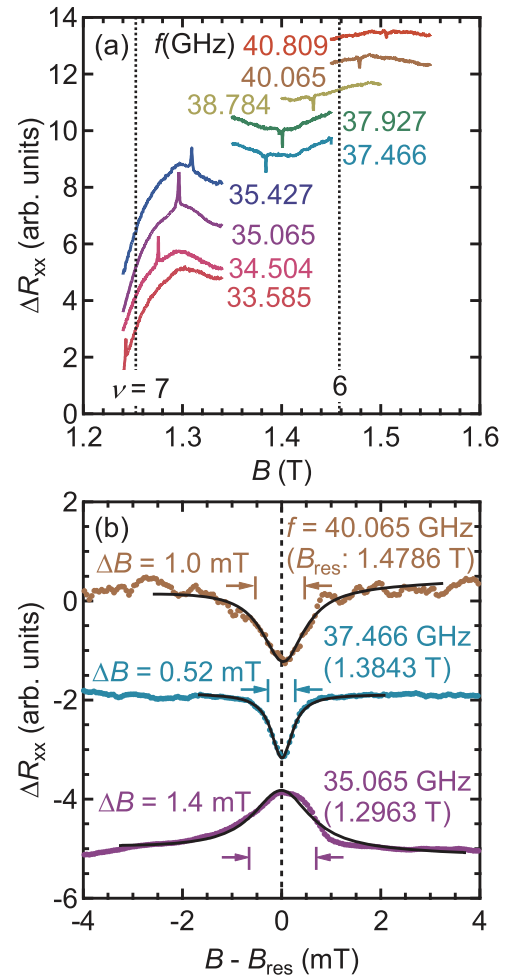


FIG. 2. (Color online) (a) The magnetic field dependence of the change in longitudinal resistance (ΔR_{xx}) in response to microwave irradiation with a variety of frequencies as indicated. ΔR_{xx} is measured by a double lock-in technique with microwave amplitude modulation in addition to alternating current modulation. The ESR signal was detected as a peak in ΔR_{xx} . (b) Three examples of ESR signal and the fitting using Eq. (1) to extract the resonance magnetic field and the transverse spin relaxation time. The full widths at half maximum from the fittings (ΔB) are also schematically shown.

frequency of the MW (f is the MW frequency), g^* is the effective g factor, and μ_B is the Bohr magneton.^{22–24} We did not find any hysteresis in ΔR_{xx} upon magnetic field sweep, which is observed in GaAs heterostructures as a result of dynamic nuclear spin polarization.²⁵ It is also worth noting that the residual magnetic field of the superconducting magnet is negligibly small as the ESR peaks are observed at positive and negative magnetic fields with the same absolute value. Then in order to discuss g factor and spin relaxation time, the ESR peaks are fitted by the Lorentzian function after subtracting the background as

$$\Delta R_{xx} = \frac{C_1}{(B - B_{\text{res}})^2 + C_2}, \quad (1)$$

where C_1 and C_2 are constants [Fig. 2(b)]. Although most of the ESR peaks are fitted well as shown in the top and middle curves in Fig. 2(b), a few showed an asymmetric resonance shape as in the bottom curve, which complicates the following analysis. However, this contribution to B_{res} is less than 1 mT (corresponding energy of $\sim 0.1 \mu\text{eV}$), and is negligibly small compared with the energy scale in the discussion.

In order to extract g^* , we plot microwave energy ($\hbar\omega$) as a function of B_{res} in Fig. 3(a). A nearly linear relationship results in an effective g factor ($g^* = \hbar\omega/\mu_B B_{\text{res}}$) of 1.94 at $B_{\text{res}} = 1.56$ T. This g^* value reflects the band structure and

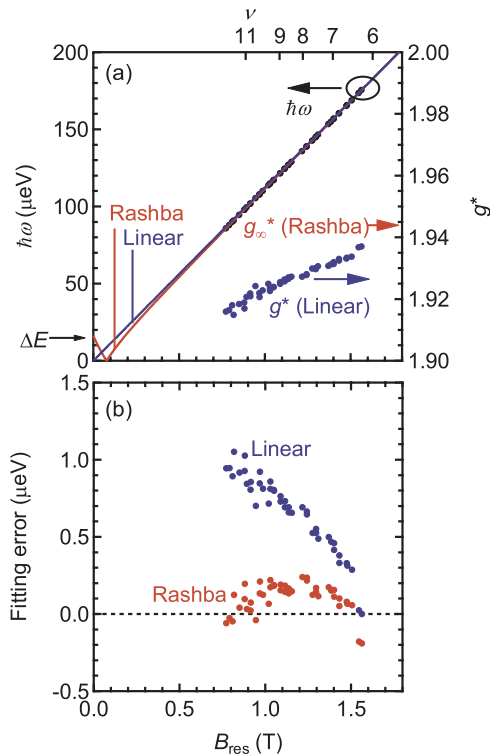


FIG. 3. (Color online) (a) Microwave energy at the resonance condition ($\hbar\omega$) as a function of resonance magnetic field (B_{res}) (black circles). The data are fitted by a linear function ($g^*\mu_B B_{\text{res}}$, blue curve) and by a function including Rashba term [Eq. (2), red curve]. The effective g factor ($g^* = \hbar\omega/\mu_B B_{\text{res}}$) and the g factor in the high-field limit (g_∞^*) estimated by the fitting with Eq. (2) are also shown on the right axis. (b) The errors between the experimental data and the two kinds of fittings shown in (a) as a function of B_{res} .

SOI of the 2DEG, and is free from an enhancement by electron correlation²⁶ as reported in previous tilted field transport experiments.²⁷ In this respect, the g^* value is almost consistent with previous ESR and optical studies on (Mg)ZnO bulk crystals and thin films.^{28,29} At lower B_{res} , however, g^* shows a small but nontrivial systematic deviation from the fitting, which is evident by subtracting the resonant $\hbar\omega$ from the fitting line with $g^* = 1.94$ as shown in Fig. 3(b). Although a similar magnetic field dependent g^* has been reported for GaAs 2DEG heterostructures as a signature of nonparabolicity in the band structure, our result cannot be interpreted in this way. In this scenario, g^* is described by $g_0 + c(N + 1/2)B$ (g_0 and c are constants, and N is the Landau level index), and shows Landau level dependent oscillations.^{30,31} However, such oscillations are not observed in our MgZnO/ZnO heterostructure as shown in Fig. 3(a). Instead, our result may be explained by including Rashba SOI, where spin-split Landau levels are expressed as³²

$$E_{N\pm} = \hbar\omega_c \left(N + \frac{1}{2} \pm \frac{1}{2} \right) \mp \frac{1}{2} \sqrt{(\hbar\omega_c - g_\infty^* \mu_B B)^2 + 8\alpha^2 \frac{eB}{\hbar} \left(N + \frac{1}{2} \pm \frac{1}{2} \right)}. \quad (2)$$

Here we use our evaluated $m^* = 0.456m_0$ in $\omega_c = eB/m^*$ and approximated N of $\pi\hbar n/eB$. The fitting of $\hbar\omega$ by $|E_{N+} - E_{N-}|$ results in much smaller fitting error than the linear fitting as shown in Fig. 3(b), although small residual error is still evident, the origin of which is currently not clear. From the fitting we obtained α and g_∞^* values of 7.0×10^{-14} eV m and 1.94, respectively, and the corresponding zero-field spin splitting (ΔE) of $2\alpha k_F = 16 \mu\text{eV}$ ($k_F = \sqrt{2\pi n}$ is the Fermi wave number). In general, Dresselhaus SOI, which originates from bulk inversion asymmetry, also contributes to spin splitting. However, previous calculation for bulk ZnO showed that Rashba effect is larger at low carrier density regime ($n < \sim 10^{13} \text{ cm}^{-2}$) as in the present case.³³ Since Rashba effect may be even larger at the heterointerface than in bulk, we neglected Dresselhaus SOI in this analysis.

The obtained α follows the Si/SiGe (5.5×10^{-15} eV m) heterostructure as the second smallest in magnitude among prevalent semiconductor heterostructures. In contrast, the α value is smaller by a few orders of magnitude than those of (In,Ga)As/(In,Al)As heterostructures with relatively strong SOI.^{5,9} Therefore, a long T_2^* may be expected, given the weak Rashba SOI as well as low nuclear spin density. T_2^* was then estimated from the FWHM of the ESR peaks^{23,34} as $T_2^* = 2\hbar/g^*\mu_B \Delta B$ ($\Delta B = 2\sqrt{C_2}$ is the FWHM of the resonance peak) from the fitting shown in Fig. 2(a). As other contributions such as longitudinal spin relaxation time (T_1) could affect the resonance linewidth, we take T_2^* as the lower bound of the real transverse spin relaxation time (T_2) although $T_1 > T_2$ is always fulfilled and T_2 is usually the most dominant for the broadening. As shown in Fig. 4, T_2^* is plotted as a function of B_{res} , exhibiting a maximum T_2^* value of 27 ns and an enhancement at several magnetic fields. Such behavior is reminiscent of SdH oscillations as a function of B_{res} (Refs. 35–37), however the enhancement does not exactly

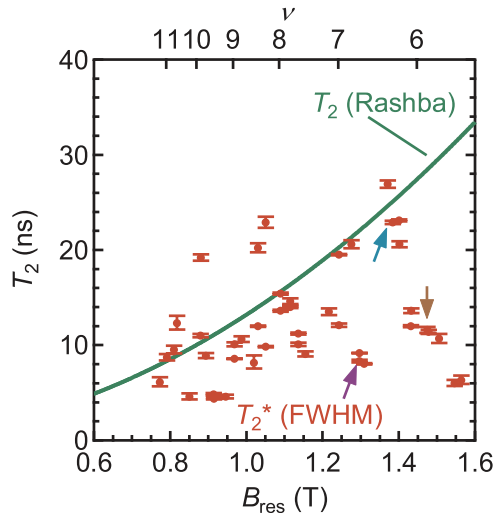


FIG. 4. (Color online) Transverse spin relaxation time as a function of resonance magnetic field with error bars obtained from the fitting results. The contribution of the Rashba effect estimated from Eq. (3) is also shown by the green curve. The arrows indicate the points shown in (a).

match the integer filling factors and is not discussed here in detail.

In Fig. 4(b) the expected spin relaxation time from the DP process is displayed as the solid line $T_2(\text{Rashba})$, which is calculated by¹⁰

$$\frac{1}{T_2(\text{Rashba})} = \frac{\alpha^2 k_F^2 \tau_p}{\hbar^2} \frac{2}{1 + (\omega_L - \omega_c)^2 \tau_p^2}, \quad (3)$$

where $\tau_p = m^* \mu / e$ is the momentum relaxation time, ω_L ($=\omega$ at the resonance) is the Larmor frequency. As shown in Fig. 4(b), $T_2(\text{Rashba})$ is roughly consistent with the experimental T_2^* , but noticeable deviations arise at higher magnetic field, suggesting the presence of another dominating component. Such mechanisms may include SOI via momentum relaxation (Elliot-Yafet, EY), electron-hole interaction (Bir-Aronov-Pikus), and the interaction with a small number of nuclear spins. The EY contribution was calculated to small

compared with DP,³⁸ while electron-hole interaction is also not relevant in our experiment because of the absence of holes. Thus, the contribution of nuclear spin has to be considered. In recent work, the spin relaxation was recently examined in colloid ZnO nanoparticles, where SOI is absent, leading to a T_2^* evaluation of about 25 ns in the presence 4% ^{67}Zn (Ref. 39). A similar value has also been reported for ZnO thin films and bulk crystals by time-resolved optical experiments.²⁸ Thus, nuclear spin may also be comparatively dominant in our MgZnO/ZnO heterostructure when the Rashba contribution is suppressed at high magnetic field.³⁶

IV. CONCLUSIONS

In conclusion, we have studied Rashba spin-orbit interaction and spin relaxation time using electrically detected electron spin resonance. Our result provides the first experimental determination of Rashba parameter of 7.0×10^{-14} eV m. Among the widely studied currently available heterostructures, this value is the second lowest, following the Si/SiGe system (5.5×10^{-15} eV m).¹⁹ The spin relaxation time was also evaluated as a maximum value of 27 ns. The spin relaxation was found to be partly limited by the Rashba effect, but other contributions such as nuclear spins may become dominant at high magnetic field in particular. Nevertheless, the extremely high electron mobility of the system may enable spin diffusion lengths on the order of $\sim 40 \mu\text{m}$, providing a promising platform for spintronic applications.

ACKNOWLEDGMENTS

We acknowledge Y. Kasahara and Y. Iwasa for useful discussions. This work was partly supported by Grant-in-Aids for Scientific Research (S) No. 24226002 and Grant-in-Aid for Scientific Research on Innovative Areas No. 21102003 from MEXT, Japan, and by ‘‘Funding Program for World-Leading Innovative R&D on Science and Technology (FIRST)’’ Program from the Japan Society for the Promotion of Science (JSPS) initiated by the Council for Science and Technology Policy as well as by Murata Science Foundation (Y.K.).

*kozuka@ap.t.u-tokyo.ac.jp

¹I. Žutić, J. Fabian, and S. D. Sarma, *Rev. Mod. Phys.* **76**, 323 (2004).

²D. D. Awschalom and M. E. Flatté, *Nat. Phys.* **3**, 153 (2007).

³M. I. Dyakonov, ed., *Spin Physics in Semiconductors* (Springer, Berlin, 2008).

⁴E. I. Rashba, *Fiz. Tverd. Tela (Leningrad)* **2**, 1224 (1960) [*Sov. Phys. Solid State* **2**, 1109 (1960)].

⁵J. Nitta, T. Akazaki, H. Takayanagi, and T. Enoki, *Phys. Rev. Lett.* **78**, 1335 (1997).

⁶M. Duckheim and D. Loss, *Nat. Phys.* **2**, 195 (2006).

⁷M. Kohda, S. Nakamura, Y. Nishihara, K. Kobayashi, T. Ono, J. Ohe, Y. Tokura, T. Mineno, and J. Nitta, *Nat. Commun.* **3**, 1082 (2012).

⁸M. I. D’yakonov and V. I. Perel’, *Fiz. Tverd. Tela (Leningrad)* **13**, 3581 (1971) [*Sov. Phys. Solid State* **13**, 3023 (1972)].

⁹T. Koga, J. Nitta, T. Akazaki, and H. Takayanagi, *Phys. Rev. Lett.* **89**, 046801 (2002).

¹⁰M. Fanciulli, ed., *Electron Spin Resonance and Related Phenomena in Low Dimensional Structures* (Springer, Berlin, 2009).

¹¹B. M. Maune, M. G. Borselli, B. Huang, T. D. Ladd, P. W. Deelman, K. S. Holabird, A. A. Kiselev, I. Alvarado-Rodriguez, R. S. Ross, A. E. Schmitz, M. Sokolich, C. A. Watson, M. F. Gyure, and A. T. Hunter, *Nature (London)* **481**, 344 (2012).

¹²L. C. Lew Yan Voon, M. Willatzen, M. Cardona, and N. E. Christensen, *Phys. Rev. B* **53**, 10703 (1996).

¹³A. Tsukazaki, A. Ohtomo, T. Kita, Y. Ohno, H. Ohno, and M. Kawasaki, *Science* **315**, 1388 (2007); A. Malashevich and D. Vanderbilt, *Phys. Rev. B* **75**, 045106 (2007).

¹⁴A. Tsukazaki, S. Akasaka, K. Nakahara, Y. Ohno, H. Ohno, D. Maryenko, A. Ohtomo, and M. Kawasaki, *Nat. Mater.* **9**, 889 (2010); Y. Kozuka, A. Tsukazaki, D. Maryenko, J. Falson,

- S. Akasaka, K. Nakahara, S. Nakamura, S. Awaji, K. Ueno, and M. Kawasaki, *Phys. Rev. B* **84**, 033304 (2011); D. Maryenko, J. Falson, Y. Kozuka, A. Tsukazaki, M. Onoda, H. Aoki, and M. Kawasaki, *Phys. Rev. Lett.* **108**, 186803 (2012); Y. Kasahara, Y. Oshima, J. Falson, Y. Kozuka, A. Tsukazaki, M. Kawasaki, and Y. Iwasa, *ibid.* **109**, 246401 (2012).
- ¹⁵J. Falson, D. Maryenko, Y. Kozuka, A. Tsukazaki, and M. Kawasaki, *Appl. Phys. Express* **4**, 091101 (2011).
- ¹⁶S. Datta and B. Das, *Appl. Phys. Lett.* **56**, 665 (1990).
- ¹⁷D. Loss and D. P. DiVincenzo, *Phys. Rev. A* **57**, 120 (1998).
- ¹⁸S. Schmult, M. J. Manfra, A. Punnoose, A. M. Sergent, K. W. Baldwin, and R. J. Molnar, *Phys. Rev. B* **74**, 033302 (2006).
- ¹⁹Z. Wilamowski, W. Jantsch, H. Malissa, and U. Rössler, *Phys. Rev. B* **66**, 195315 (2002).
- ²⁰R. Meisels, I. Kulac, F. Kuchar, and M. Kriechbaum, *Phys. Rev. B* **61**, 5637 (2000).
- ²¹L. Smrčka, H. Havlova, and A. Isihara, *J. Phys. C* **19**, L475 (1986).
- ²²D. Stein, K. v. Klitzing, and G. Weimann, *Phys. Rev. Lett.* **51**, 130 (1983).
- ²³C. F. O. Graeff, M. S. Brandt, M. Stutzmann, M. Holzmann, G. Abstreiter, and F. Schäffler, *Phys. Rev. B* **59**, 13242 (1999).
- ²⁴J. Matsunami, M. Ooya, and T. Okamoto, *Phys. Rev. Lett.* **97**, 066602 (2006).
- ²⁵S. Teraoka, A. Numata, S. Amaha, K. Ono, and S. Tarucha, *Physica E* **21**, 928 (2004).
- ²⁶J. F. Janak, *Phys. Rev.* **178**, 1416 (1969).
- ²⁷A. Tsukazaki, A. Ohtomo, M. Kawasaki, S. Akasaka, H. Yuji, K. Tamura, K. Nakahara, T. Tanabe, A. Kamisawa, T. Gokmen, J. Shabani, and M. Shayegan, *Phys. Rev. B* **78**, 233308 (2008); Y. Kozuka, A. Tsukazaki, D. Maryenko, J. Falson, C. Bell, M. Kim, Y. Hikita, H. Y. Hwang, and M. Kawasaki, *ibid.* **85**, 075302 (2012).
- ²⁸S. Ghosh, V. Sih, W. H. Lau, D. D. Awschalom, S.-Y. Bae, S. Wang, S. Vaidya, and G. Chapline, *Appl. Phys. Lett.* **86**, 232507 (2005); S. Ghosh, D. W. Steuerman, B. Maertz, K. Ohtani, H. Xu, H. Ohno, and D. D. Awschalom, *ibid.* **92**, 162109 (2008).
- ²⁹T. A. Wassner, B. Laumer, M. Althammer, S. T. B. Goennenwein, M. Stutzmann, M. Eickhoff, and M. S. Brandt, *Appl. Phys. Lett.* **97**, 092102 (2010).
- ³⁰G. Lommer, F. Malcher, and U. Rössler, *Phys. Rev. B* **32**, 6965 (1985).
- ³¹M. Dohers, K. v. Klitzing, and G. Weimann, *Phys. Rev. B* **38**, 5453 (1988).
- ³²R. Winkler, *Spin-Orbit Coupling Effects in Two-Dimensional Electron and Hole Systems* (Springer, Berlin, 2003).
- ³³J. Y. Fu and M. W. Wu, *J. Appl. Phys.* **104**, 093712 (2008).
- ³⁴Z. Wilamowski and W. Jantsch, *Phys. Rev. B* **69**, 035328 (2004).
- ³⁵V. Sih, W. H. Lau, R. C. Myers, A. C. Gossard, M. E. Flatté, and D. D. Awschalom, *Phys. Rev. B* **70**, 161313(R) (2004).
- ³⁶A. A. Burkov and L. Balents, *Phys. Rev. B* **69**, 245312 (2004).
- ³⁷D. Fukuoka, T. Yamazaki, N. Tanaka, K. Oto, K. Muro, Y. Hirayama, N. Kumada, and H. Yamaguchi, *Phys. Rev. B* **78**, 041304(R) (2008).
- ³⁸N. J. Harmon, W. O. Putikka, and R. Joynt, *Phys. Rev. B* **79**, 115204 (2009).
- ³⁹K. M. Whitaker, S. T. Ochsenbein, A. L. Smith, D. C. Echodu, B. H. Robinson, and D. R. Gamelin, *J. Phys. Chem. C* **114**, 14467 (2010).